Experimental and numerical investigation of the bending capacity of spiral-welded steel tubes

van Es, Sjors; Gresnigt, Nol; Vasilikis, D; Karamanos, SA

Publication date
2016

Document Version
Accepted author manuscript

Published in
Proceedings of the International Colloquium on Stability and Ductility of Steel Structures

EXPERIMENTAL AND NUMERICAL INVESTIGATION OF THE BENDING CAPACITY OF SPIRAL-WELDED STEEL TUBES

Sjors H.J. van Es[a], Arnold M. Gresnigt[a], Daniel Vasilikis[b] and Spyros A. Karamanos[b]

[a] *Delft University of Technology, Delft, The Netherlands*
[b] *University of Thessaly, Volos, Greece*

Abstract: To investigate the structural behaviour of large-diameter spiral-welded steel tubes under bending, a full scale experimental program has been performed, consisting of thirteen 42-inch diameter, spiral-welded steel tubes with D/t ratios ranging between 65 and 120. Additionally, numerical studies have been conducted, using nonlinear finite element simulations. A model has been developed to simulate the performed tests, using the actual material properties and initial geometric imperfections obtained from the tested tubes. Finally, a parametric investigation has been performed that investigates the influence of initial geometric imperfections and presence of girth and coil connection welds on the bending behaviour of the considered tubes.

1. Introduction

The spiral-welding manufacturing process (HSAW) offers an economical method to manufacture relatively thin-walled, large-diameter steel tubes. An overview of this manufacturing process is presented in Fig. 1a. Common tube diameters (D) range from 500 mm to 3000 mm with wall thicknesses (t) between 9 mm and 25 mm. The process is continuous; a steel coil that runs out is connected to a new coil by means of a butt weld without interruption of the spiral-welding process. This weld, running perpendicular to the spiral welds, is denoted as a coil-connection weld (CCW). Aside from this coil connection weld, girth welds (GW) occur in structures when two separate tubes are joined (see Fig. 1b).

Large-diameter spiral-welded tubes are employed in for example hydrocarbon and water pipelines, but also in structural applications. The present research mainly focuses on the behaviour of spiral-welded tubes for application in combined walls. In these soil retaining structures, large diameter, thin-walled tubes are used as primary structural elements to resist horizontal soil loads. Steel tubes used in these applications are generally manufactured with

the spiral-welding process. Due to the slenderness of the tubes that are typically applied in these structures, local buckling is the dominating failure mode.

The pure bending response of metal tubes has been investigated numerous times in the last decades, yet investigations focusing on spiral-welded tubes are scarce. In [1], four bending tests are performed on spiral-welded tubes with D/t=48 and 82, intended for linepipe use. Therefore, two of these tests were conducted with internal pressure in the tube. In [2], a similar testing programme is conducted on four spiral welded tubes with D/t=46 and 64. Both studies deem the performance of the tubes to be satisfactory but neither includes the presence of girth welds or coil connection welds. Eight bending tests on more thin-walled spiral-welded tubes have been performed by Reinke et al. [3], as part of the same project as the present research. Also in the tests by Reinke et al., the spiral welded tubes performed well. The spiral weld was deemed to have no influence on the maximum bending moment capacity of the specimens; deformation capacity was not investigated.

The current research is part of a research project with acronym COMBITUBE, which examines the bending behaviour of large-diameter steel tubes, specifically for application in combined walls [4].

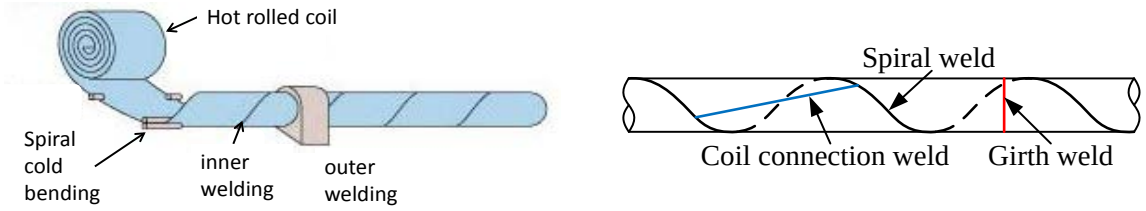

a) Spiral-welding manufacturing process b) CCW and GW in a spiral-welded tube

Fig. 1: Overview of spiral welding manufacturing process and resulting welds in spiral-welded tubes

2. Experimental work

2.1 Overview

The testing program featured investigation of the initial geometry and geometrical imperfections, extensive material testing and four-point bending tests on thirteen 42-inch diameter (1067 mm) spiral-welded carbon steel tubes.

The length of all specimens was 16500 mm. The D/t ratios varied from 65 to 120 and the steel grades varied from X52 to X70 (see Table 1). The experimental program includes plain tubes that feature only a spiral weld, but also tubes with additional welds such as girth welds and coil connection welds. If present, these welds divided a specimen in two or more sections which are referred to as ‘specimen parts’ and are identified by adding the indicators ‘left’, ‘middle’ and ‘right’ to the specimen identification.

2.1 Measurement of initial geometry and geometrical imperfections

The tube diameter and wall thickness have been measured at five cross sections along the tube in 45 degree increments of axial tube rotation. Additionally, the wall thickness variation across the width of the original coiled steel plate has been investigated by taking measurements along a line perpendicular to the spiral weld. The wall thickness measurements were performed using an ultrasonic thickness measurement device. The geometric profile of the tube wall has been scanned using a laser trolley driving on rails below the specimen. An overview of this test setup is depicted in Fig. 2.

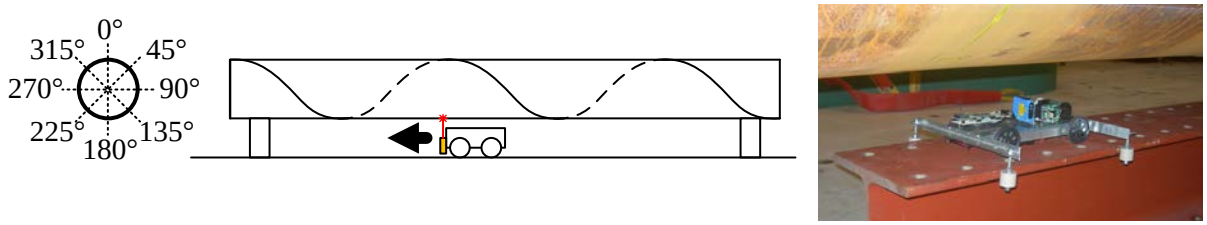

a) Schematic overview b) Photograph of laser trolley

Fig. 2: Overview of test setup for measurement of geometrical imperfections

2.2 Four-point bending tests

To determine the maximum bending capacity of the tubes, the specimens were loaded in four-point bending by applying an upward displacement at the two outer supports (see Fig. 3). Due to limited availability of hydraulic actuators in the laboratory, different actuators were used on each side of the tube. Despite this difference, the loading on the specimen itself was symmetric. After local buckling failure, deformation was further increased until the full stroke of the actuators was used.

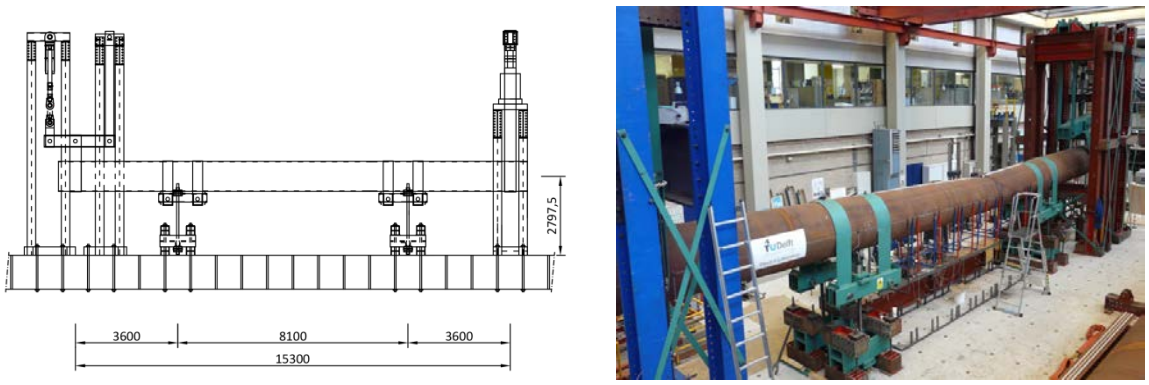

a) Schematic overview b) General view of test setup

Fig. 3: Overview of four-point bending test setup

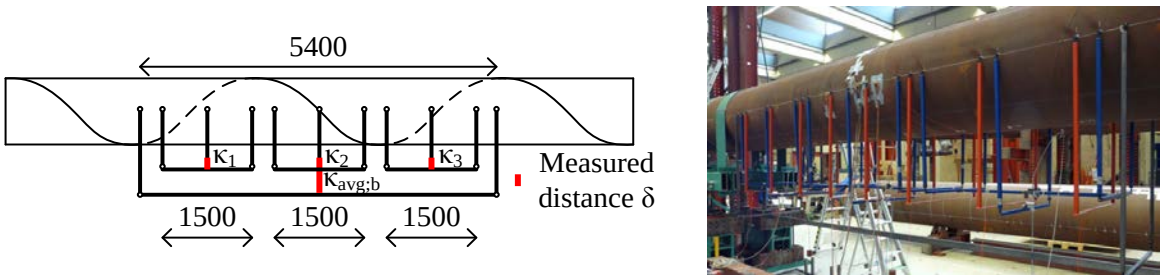

a) Schematic overview b) Photograph of measurement brackets

Fig. 4: Overview of curvature measurements using brackets

During the tests, the applied displacements and the resulting forces were measured continuously. Furthermore, the curvature (κ) of the tube was measured over three tube segments with a length L of 1500 mm, and over the full tube segment that was loaded in constant bending moment. Each curvature measurement used three brackets, of which the outer two were coupled (see Fig. 4). From the measured distance δ between the centre bracket and the coupler bar, the curvature of the examined tube section was calculated using Eq. (1). A more elaborate description of the performed measurements can be found in [5].

$$\kappa = \frac{8 \cdot \delta}{L^2} \tag{1}$$

3. Results of experiments

3.1 Results of measurements of tube geometry and initial geometrical imperfections

The scans of the initial geometry of the tubes show a very regular imperfection pattern. Between the spiral welds a regular pattern of wave-like shapes occurs in all investigated tubes (see Fig. 5). In some of the tubes, the outer surface showed markings, caused by the rolling equipment used to bend a tube from the coiled steel plate. Since these markings align with the amplitudes in the imperfection profiles, the imperfections profile is assumed to originate from the spiral-welding process. Near girth welds and coil connection welds, more local and generally larger geometrical imperfections occur. A more thorough discussion of all geometrical imperfections and their origins can be found in [5] and [6].

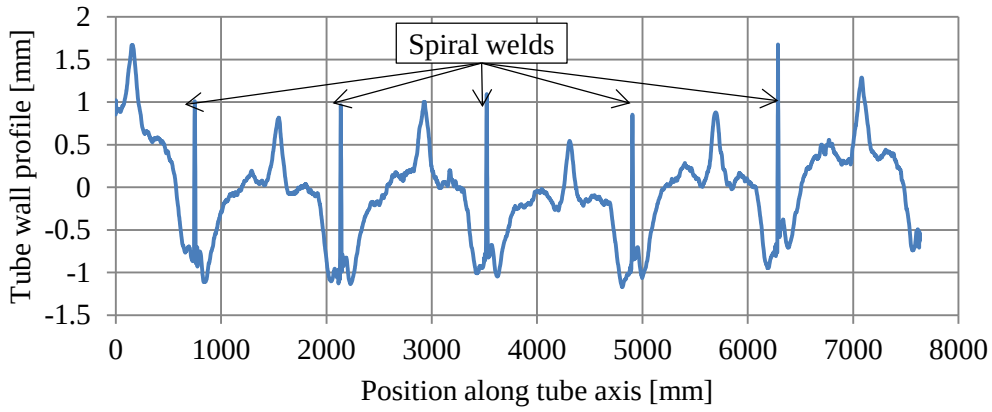

Fig. 5: Example of measured initial geometrical imperfection profile (Tube T2)

The average wall thickness of each specimen is listed in Table 1. The variation of the wall thickness within the specimen parts was found to be very small and is therefore neglected in the following analyses. The measurements over a line perpendicular to a spiral weld have shown a decrease in wall thickness towards the spiral welds of about 1%. This is also considered to be negligible.

The diameter of the tubes was very close to the specified value of 1067 mm. Aside from the average diameter, the initial ovalisation of the tube is recognized as a relevant parameter. The initial ovalisation f is defined as $(D_{max}-D_{min})/D_{ave}$. This parameter was estimated using the diameters measured in 45° increments (see section 2.2). The results show that only one of the tubes exceeds an initial ovalisation of 0.5%, which is considered to be excellent.

3.2 Results of four point bending tests

As a result of the exerted bending loads, all tubular specimens failed in the form of local buckling. The specimens with D/t=120 failed suddenly and violently. In contrast, the transition between a stable and unstable situation was much more gradual for the thicker walled tubes. The violent failure of the thin walled tubes in some cases resulted in failure of the measurement equipment. If this occurred, graphical representations of measurements are truncated at the moment of failure. Examples of failed specimens are presented in Fig. 6.

The main output of the bending tests is the moment-curvature (M-κ) diagram. Since four different curvature measurements were used, each test results in four diagrams. Results of two typical tests are presented in Fig. 7. The results show that in the inelastic part of the moment-curvature response, the four curvature measurements show different results. For example, the

curvature measured by measurement κ_1 is significantly higher than the others in Fig. 7a. Apparently, the curvature is not constant within the tube segment that is loaded by a constant bending moment, caused by variations in bending resistance over the length of the tube. The moment-curvature diagrams further show that these tubes did not fail in elastic buckling. Instead, an elasto-plastic buckling mode develops.

a) Test result of test T7 b) Test result of test T2 c) FEA result of test T2

Fig. 6: Examples of local buckles in spiral-welded tubular specimens

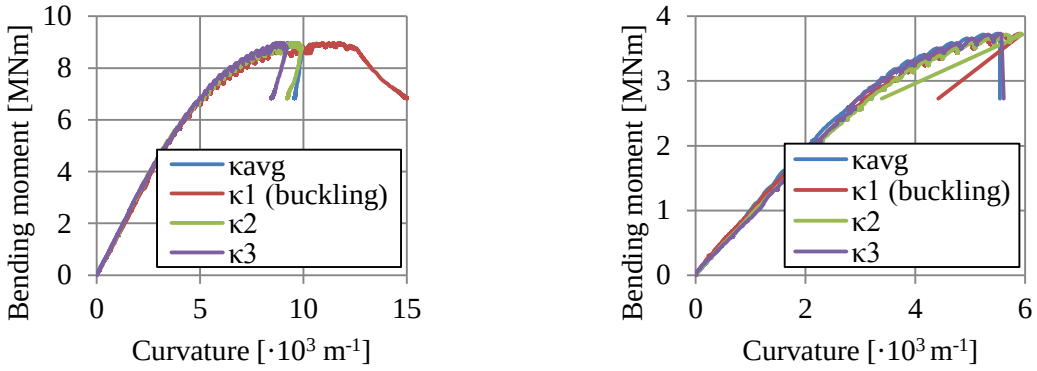

a) Specimen T9 (D/t=65.4) b) Specimen T4 (D/t=116)

Fig. 7: Moment-curvature diagrams of typical specimens. Local buckling takes place within the local measurement marked with '(buckling)'

The critical curvature κ_{cr} is defined as the measured average curvature at the occurrence of the maximum bending moment. An overview of the reached critical compressive strains (ε_{cr}), determined from the critical curvatures, is presented in Fig. 8a. The figure shows that specimens containing a girth weld or coil connection weld exhibit a slightly lower critical strain. It is assumed that is the result of e.g. misalignments at the weld and discontinuities in bending moment capacity, which result in concentration of deformation. The maximum resisted bending moment, normalized by the full plastic bending moment (M_{pl}), is presented in Fig. 8b for each specimen. The slenderness is normalized by $D/(t\varepsilon^2)$, with $\varepsilon^2=235/\sigma_y$, as suggested by [7]. Specimens containing a girth weld or coil connection weld appear to have a lower or equal bending moment capacity than plain specimens. Exception to this trend is specimen T10. Local buckling occurred at one side of the girth weld, on the opposite side of the weld a 50% higher yield strength was measured. Apparently the negative effect of the girth weld was counteracted by a positive effect of this yield strength difference.

In all plain specimens, local buckling occurred at the manufacturing-related geometrical imperfections. None of the buckles formed directly at a spiral weld. The presence of a girth weld or coil connection weld resulted in local buckling at this weld in four out of six cases.

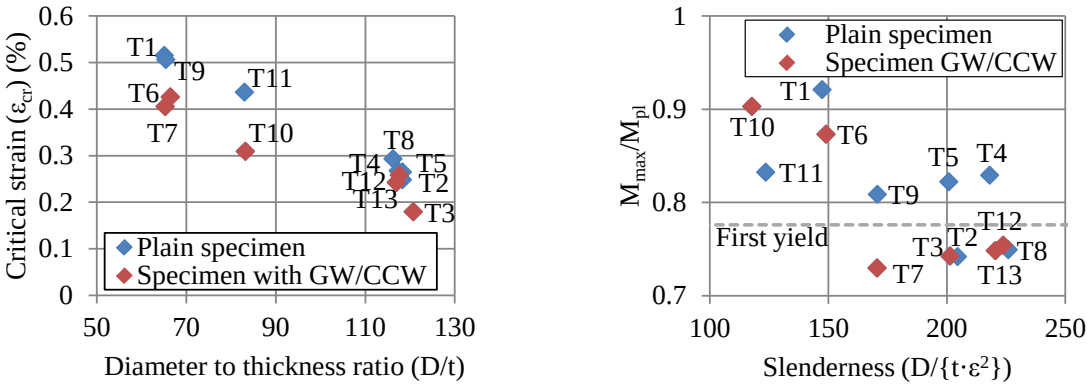

a) Critical strains b) Normalized maximum bending moments

Fig. 8: Overview of test results of four point bending tests

4. Numerical simulation of four point bending tests

4.1 Results of four point bending tests

A numerical model has been developed in ABAQUS/Standard [8]. The tubes are modelled with four-node reduced integration shell elements (S4R). Inelastic material behaviour is considered using a Von Mises plasticity model with isotropic hardening. Residual stresses are inserted in the model to simulate the effects of the manufacturing process of spiral welded tubes [9].

For the simulation of plain tubes, a dense rectangular mesh of elements is employed (Fig. 9a), with an element size equal to 50 mm. The tube is initially imperfect, with a wavy-type (wrinkling) geometric imperfection, in the form of the first buckling mode (Fig. 9b) with amplitude δ_0. Seven elements are present per half-wavelength. In case of a tube with a girth weld, different material properties are taken into account on each side of the weld.

Four reference nodes have been introduced to represent the bending test set-up; two reference points refer to the supports and two to the locations where forces are applied (see Fig. 10). An arc-length continuation algorithm (Riks) is employed to trace the load-displacement path.

a) Rectangular finite element mesh of initially wrinkled tube (magnified for visualization purposes) b) Initially wrinkled pattern in the compression side

Fig. 9: Overview of FEA model for plain tubes and definition of geometrical imperfections

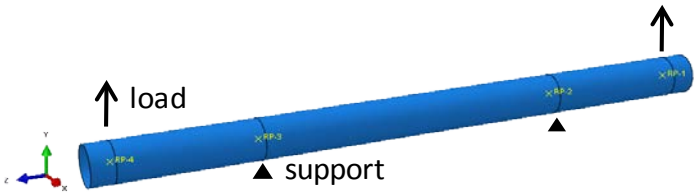

Fig. 10: Numerical model of four-point bending in ABAQUS

In addition to the rectangular mesh of Fig. 9, a "spiral mesh" has also been employed (see Fig. 11a) with similar density. In that mesh, the spiral weld is modelled as a separate part, with different material properties, so that over-matching of the spiral weld is considered. In case of tubes containing girth and/or coil connection welds, the tube is divided in parts with separate geometric and material properties (Fig. 11b).

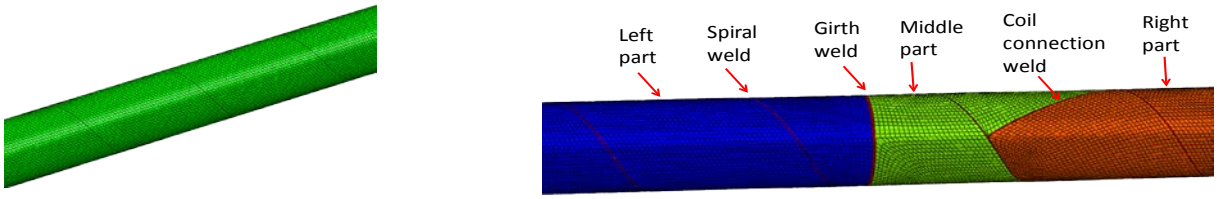

a) Spiral mesh for the analysis of spiral-welded tubes

b) Partitioning and meshing of a tube containing both girth and coil connection weld

Fig. 11: Overview of FEA model with spiral mesh, suitable for modelling of coil connection welds

4.2 Numerical results

The comparison between numerical and experimental results for all tests is presented in the last four columns of Table 1, whereas moment-curvature diagrams for two representative tests are depicted in Fig. 12. The bending curvature reported in the numerical results is calculated as the sum of the two rotations at the middle supports, averaged over the initial distance between the two supports. Moment values are normalized by the plastic bending moment, and bending curvature is normalized by the curvature-like quantity $\kappa_I=t/D_m^2$. The results from Fig. 12 and Table 1 show a very good comparison between the numerical results and the experimental data, and indicate that the developed models are able to accurately predict the bending response of spiral welded tubes in terms of both ultimate bending moment capacity and deformation capacity. In all cases, the buckled shapes obtained numerically are in excellent agreement with the shapes observed in the experiments (e.g. see Fig. 6b and c).

Table 1: Summary of bending tests; comparison between numerical and experimental results

Test	Type	Geometric data			Yield stress	Initial wrinkle	Moment (M_{max}/M_{pl})		Curvature κ_{cr}/κ_I	
		D [mm]	t [mm]	D/t [-]	σ_y [MPa]	δ_0/t [%]	Test [-]	FEM [-]	Test [-]	FEM [-]
T1	Plain	1066	16.4	65.1	541	1.8	0.907	0.940	0.646	0.694
T2	Plain	1067	9.02	118	392	4.5	0.769	0.842	0.559	0.669
T4	Plain	1065	9.16	116	420	3.0	0.871	0.845	0.761	0.713
T5	Plain	1070	9.04	118	403	3.6	0.814	0.852	0.681	0.762
T8	Plain	1068	9.10	117	435	5.8	0.781	0.807	0.697	0.691
T9	Plain	1069	16.30	65.4	571	4.6	0.869	0.935	0.696	0.819
T11	Plain	1068	12.90	83.0	341	3.1	0.865	0.945	0.726	0.728
T3	GW	1069	9.03	118	392	10.0	0.735	0.771	0.432	0.510
T13	GW	1070	9.18	116	443	12.8	0.744	0.772	0.633	0.612
T6	CCW	1066	16.30	65.3	528	9.3	0.876	0.941	0.586	0.631
T7	CCW+GW	1068	16.30	65.4	614	5.5	0.730	0.903	0.533	0.705
T10	CCW+GW	1070	13.1	81.6	333	13.7	0.897	0.916	0.480	0.498
T12	CCW+GW	1069	9.13	117	431	6.7	0.783	0.815	0.690	0.706

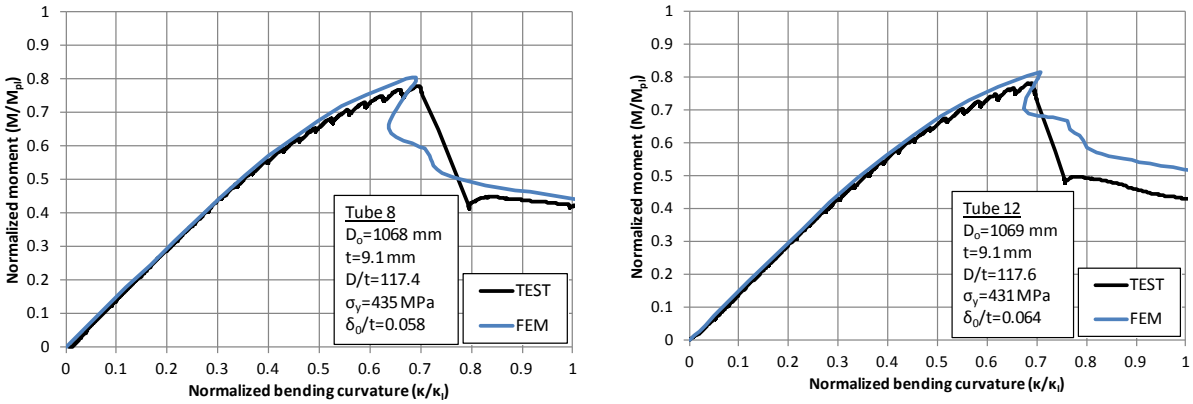

a) Specimen T8 b) Specimen T12

Fig. 12: Comparison between numerical and test results in terms of moment-curvature curves

5. Numerical parameter study

5.1 Wrinkling imperfections sensitivity

Numerical results that investigate the imperfection sensitivity of the bending response are presented in Fig. 13 for 42-inch-diameter tubes with D/t=67 and 119 respectively, in the absence of residual stresses. The results show that both the maximum bending moment and critical curvature are sensitive to the presence of initial wrinkles. The first tube (D/t=67) exhibits substantial inelastic deformation. For rather small values of initial imperfection amplitude (δ_0/t<0.5%), the maximum moment exceeds 95% of M_{pl}. For larger amplitudes of the initial wrinkles, the moment and deformation capacity decrease significantly. In any case, the response is characterized by a clear limit point on the moment-curvature diagram, well into the inelastic range. The thin-walled tube (D/t=119) exhibits a maximum moment less than 90% of M_{pl}. For values of δ_0/t greater than 30%, the "snap-back" in the M-κ diagram is alleviated and the response becomes smoother, characterized by a limit point.

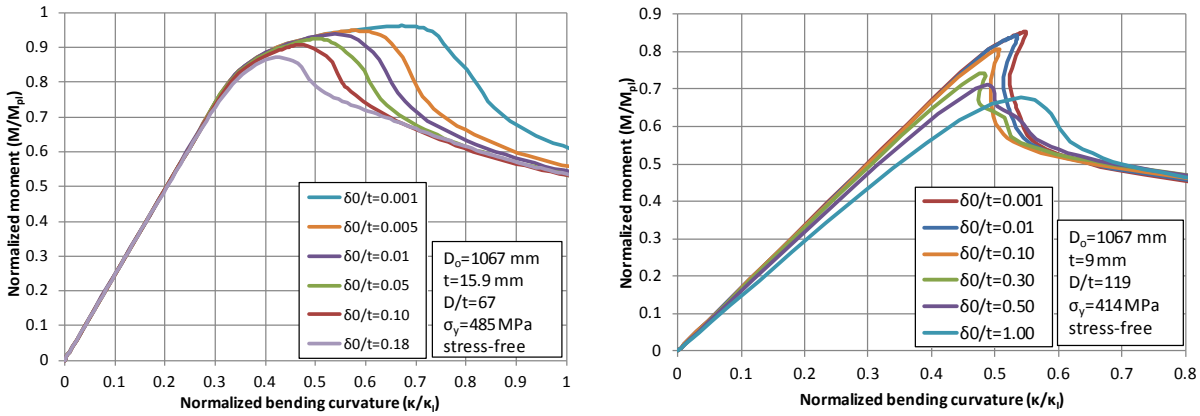

a) Tubes with D/t=67 b) Tubes with D/t=119

Fig. 13: Imperfection sensitivity of 42-inch diameter stress-free tubes subjected to bending

5.2 Effect of girth and coil connection welds

At girth welds and coil connection welds, the possible discontinuity in material properties of the two connected tubes may result in stress and strain concentrations, facilitating the formation of a local buckle. In the model, the yield stress of one part of the tube is chosen

equal to 485 MPa, while the yield stress of the other part is considered as a variable. The strength difference between the two parts is expressed as a percentage. The results in Fig. 14 indicate that significant differences in yield stress between the two connecting tube parts may decrease the critical bending curvature. This is attributed to the fact that the discontinuity in material properties acts as an imperfection, causing localization of stresses and deformation and, eventually, premature buckle formation, always in the weakest part of the tube.

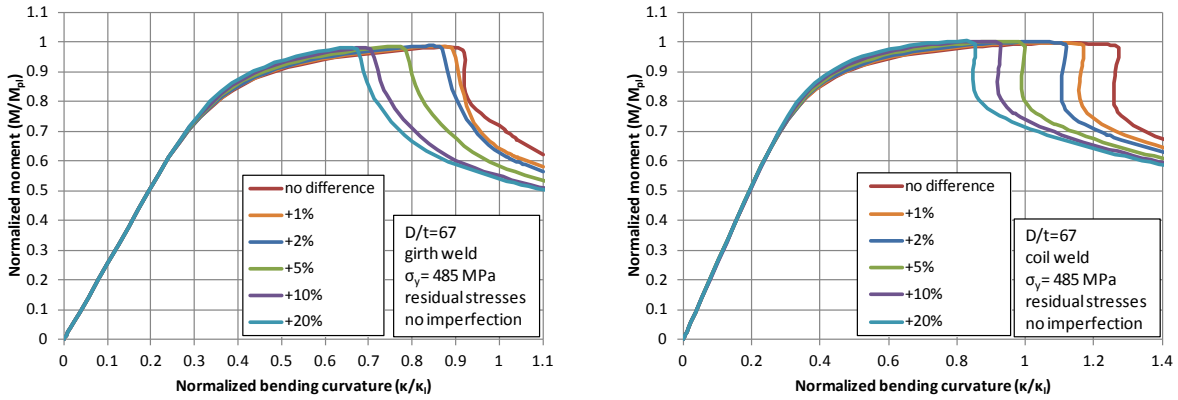

a) Tubes with girth welds b) Tubes with coil connection welds

Fig. 14: Normalized moment-curvature diagrams of a 42-inch diameter tube (*D*/*t*=67, grade X70) for different yield stress values of connected tubular parts (girth welds and coil connection welds)

5.3 Effect of girth weld misalignment

At a girth-weld, there is a possibility for eccentricity between the connected tubes. This is also referred to as “misalignment” or “high-low”. The calculated normalized critical curvature for different levels of girth weld misalignment is presented in Fig. 15. The misalignment has a considerable effect on the bending behaviour, decreasing the maximum moment and critical curvature. During bending, deformation concentrates in the girth weld region due to this misalignment, and buckling always occurs in this area in the FE-analyses. In practice, the buckling location may depend on the misalignment size and overstrength of the girth weld.

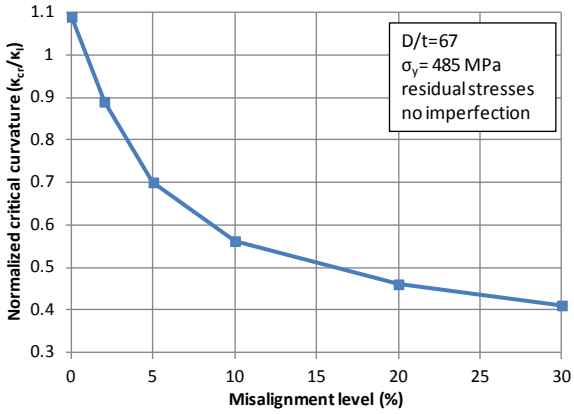

Fig. 15: Variation of normalized critical curvature in terms of the girth weld misalignment

6. Conclusions

This paper presents a summary of the results of thirteen full-scale four-point bending tests on spiral-welded steel tubes. Furthermore, a numerical study of the mechanical behaviour of these tubulars is offered using finite element models. The main findings in this paper are:

1. The tested spiral-welded tubes show regular geometrical imperfections. These imperfections are associated with the spiral-welding manufacturing method. In absence of girth welds and coil connection welds, local buckles form at such imperfections;
2. Curvature was found to be not constant over a length of tube with constant bending moment. Especially beyond the elastic range of the tube, deformation localized;
3. The presence of girth welds and coil connection welds had a penalizing effect on the critical strain and maximum resisted bending moment of the tested tubes;
4. The developed numerical model shows good comparison with experimental data in terms of moment-curvature behaviour (κ_{cr} and M_{max});
5. The tubes under consideration were found to be sensitive to initial geometrical imperfections. Even the relatively thick-walled tubes (D/t=67) show to be sensitive to realistic imperfections that were observed in the laboratory.
6. The effect of girth welds and coil connection welds is visible through the influence of a yield strength difference on either side of the weld and through misalignments at the weld itself. Both these factors can have significant influence on the critical curvature.

In [10], an analytical model is presented that is able to determine structural behaviour of these tubes, taking into account relevant parameters that determine the deformation capacity and bending moment capacity.

Acknowledgments

Funding for this work has been provided by the Research Fund for Coal and Steel (RFCS) of the European Commission, project COMBITUBE: “Bending Resistance of Steel Tubes in CombiWalls”, Grant Agreement No. RFSR-CT-2011-00034.

References

[1] Zimmerman T, Xie J, Timms C, Asante J. “Buckling resistance of large diameter spiral welded linepipe”, *Proceedings of the Int. Pipeline Conf. (IPC)*, Calgary, 2004

[2] Zimmermann S, Karbasian H, Knoop FM. “Helical Submerged Arc Welded Line Pipe Engineered For Strain Based Design”, *Proceedings of ISOPE*, Anchorage, 2013.

[3] Reinke T, Sadowski AJ, Ummenhofer T, Rotter JM. “Large Scale Bending Tests of Spiral Welded Steel Tubes”, *Proceedings of Eurosteel*, Naples, Italy, 2014.

[4] Combitube Research Group, “Bending resistance of steel tubes in CombiWalls – COMBITUBE – Final Report”, European Comission – RFCS, Brussels, 2015.

[5] Van Es SHJ, Gresnigt AM, Vasilikis D, Karamanos SA. “Ultimate Bending Capacity of Spiral-Welded Steel Tubes – Part I: Experiments”, *Thin Walled Structures, IN PRESS*

[6] Sadowski AJ, Van Es SHJ, Reinke T, Rotter JM, Gresnigt AM, Ummenhofer, T. “Harmonic analysis of measured initial geometric imperfections in large spiral welded carbon steel tubes”, *Engineering Structures*, 85, 234-248, 2015.

[7] European Committee for Standardization, “Eurocode 3: Design of steel structures – Part 1-1: General rules for buildings”, CEN, Brussels, 2006.

[8] ABAQUS, 2013. *User’ Manual*, version 6.12, Hibbitt, Karlsson and Sorensen, Inc.

[9] Vasilikis D, Karamanos SA, Van Es SHJ, Gresnigt AM. “Ultimate Bending Capacity of Spiral-Welded Steel Tubes – Part II: Predictions”, *Thin Walled Structures, IN PRESS*

[10] Gresnigt AM, Van Es SHJ, Vasilikis D, Karamanos SA. “Strain-based design procedures for spiral-welded steel tubes in combined walls”, *The International Colloquium on Stability and Ductility of Steel Structure*, Timisoara, Romania, 2016.